AMERICAN SOCIETY of
GENE & CELL
THERAPY

Effect of a Fusion Peptide by Covalent Conjugation of a Mitochondrial Cell-Penetrating Peptide and a Glutathione Analog Peptide

Carmine Pasquale Cerrato[1] and Ülo Langel[1,2]

[1]Department of Neurochemistry, Arrhenius Laboratories for Natural Sciences, Stockholm University, Svante Arrhenius väg 16B, 10691 Stockholm, Sweden; [2]Laboratory of Molecular Biotechnology, Institute of Technology, University of Tartu, Nooruse 1, 50411 Tartu, Estonia

Previously, we designed and synthesized a library of mitochondrial antioxidative cell-penetrating peptides (mtCPPs) superior to the parent peptide, SS31, to protect mitochondria from oxidative damage. A library of antioxidative glutathione analogs called glutathione peptides (UPFs), exceptional in hydroxyl radical elimination compared with glutathione, were also designed and synthesized. Here, a follow-up study is described, investigating the effects of the most promising members from both libraries on reactive oxidative species scavenging ability. None of the peptides influenced cell viability at the concentrations used. Fluorescence microscopy studies showed that the fluorescein-mtCPP1-UPF25 (mtgCPP) internalized into cells, and spectrofluorometric analysis determined the presence and extent of peptide into different cell compartments. mtgCPP has superior antioxidative activity compared with mtCPP1 and UPF25 against H_2O_2 insult, preventing ROS formation by 2- and 3-fold, respectively. Moreover, we neither observed effects on mitochondrial membrane potential nor production of ATP. These data indicate that mtgCPP is targeting mitochondria, protecting them from oxidative damage, while also being present in the cytosol. Our hypothesis is based on a synergistic effect resulting from the fused peptide. The mitochondrial peptide segment is targeting mitochondria, whereas the glutathione analog peptide segment is active in the cytosol, resulting in increased scavenging ability.

INTRODUCTION

Evidence has been accumulated over the last decades supporting the idea that reactive oxygen species (ROS) play a principal role in pathogen elimination by the microbicidal activity of phagocytes.[1] ROS have also been described to induce modifications of nucleic acids, proteins, and lipids, resulting in a crucial effect on the cell functions that may be related to the process of aging or age-related diseases.[2–5] The main sources of ROS are mitochondria, where their production is a consequence of the electron transport process. Moreover, mitochondrial dysfunction is a common event in the apoptosis mechanism leading to cell death.[6]

The ROS family consists of free radicals, such as superoxide anion ($O_2^{\cdot-}$) and hydroxyl radical ($^{\cdot}OH$), and non-radical molecules, such as hydrogen peroxide (H_2O_2) and singlet oxygen ($^1O_2$). The free radicals can be produced by oxidative reactions, leading to chain reactions causing cell damage. These chain reactions can be terminated by antioxidants via interception of the ROS, thereby limiting their toxic effects. Several antioxidants are used in vitro, in vivo, and in clinical trials, such as glutathione (GSH), vitamin E, ascorbic acid (vitamin C), and beta-carotene.[7–9]

GSH, catalase, superoxide dismutase, and other enzymes are part of a complex antioxidant system used by plants and animals to balance their oxidative state.[10] These molecules are produced internally or introduced by the diet, such as vitamin A, vitamin C, and vitamin E. It has been shown that, in some cases, the combination of two antioxidants is more effective compared with either one alone. Arlt et al.[11] showed that the dietary supplementation using a combination of vitamin C and E in Alzheimer's disease (AD) patients is a more effective treatment compared with AD patients treated with only one of them. Several recent studies have also shown controversial outcomes where dietary supplements have been suggested or found to improve health and efficiency in preventing and/or slowing the progression of different diseases.[12–18] The reduced intake and/or absorption of antioxidants from the diet and the reduced activity of endogenous antioxidative enzymes are some of the causes of decreased antioxidant defenses.[19] There are also other endogenous and exogenous factors, like inflammation, elevation in O_2 concentration, increased mitochondrial leakage, chronic inflammation, psychological and emotional stress, environmental pollution, strenuous exercise, smoking, and nutrition, that are considered causes of increased ROS production.[20]

Treatment of ROS production is also limited in terms of its physiological position. Cell membranes are usually resistant to the

CrossMark
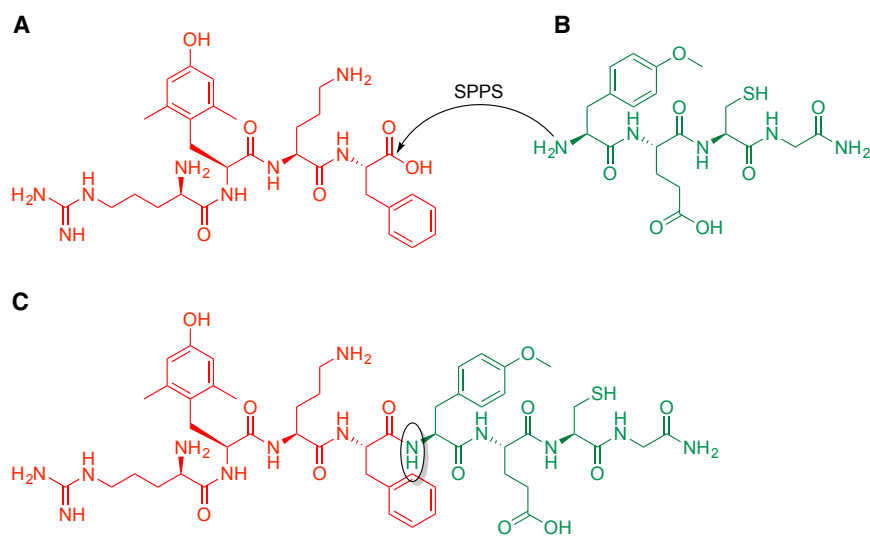
In this study, an investigation of the potential synergistic effect combining the aforementioned peptides, mtCPP1 and UPF25, is presented. The dual antioxidant peptide was developed by fusion of the mitochondrial peptide and the glutathione analog using a covalent strategy, generating a novel peptide, mtCPP1-UPF25 (mtgCPP) (Figure 1C). Our aim was to explore the potential to synergistically increase the treatment efficacy of the novel peptide acting in different compartments at the same time. This was achieved by using delivery of the fused peptide into cells, thereby increasing the therapeutic antioxidant properties and, potentially, more effectively scavenging cytoplasmic and mitochondrial ROS than either peptide alone.

RESULTS AND DISCUSSION

Solubility of Peptides

All synthesized peptides included in Table 1 were readily soluble in MilliQ water at 1 mM stock solutions. 5-(6)-carboxyfluorescein (FAM)-mtCPP1, FAM-UPF25, and FAM-mtgCPP were designed to study the intracellular uptake of peptides. The carboxyfluorescein moiety did not decrease the solubility of FAM-mtCPP1 and FAM-mtgCPP but was slightly decreased for FAM-UPF25 in MilliQ water, requiring a longer time on the vortex to have a homogeneous solution.

Effects of mtgCPP on Cell Viability

We have previously shown that mtCPP1 and UPF25 did not affect the viability of different cell lines even at high concentration (100 μM).[27,28] We compared the effects of mtgCPP at different concentrations on the viability of HeLa 705 cells after 24 hr (Figure 2). A solution of 20% DMSO in complete cell growth medium was used to treat cells as a positive control. Cell viability was registered to be approximately 20%. mtgCPP did not show any significant toxic effects on the viability of HeLa 705 cells, nor did the other peptides at any of the tested concentrations (1, 5, 10, 20, 50, and 100 μM). Furthermore, we studied the effects of the same set of peptides and concentrations on the viability of Chinese hamster ovary (CHO), bEnd.3 (mouse brain endothelial), and U87 (human brain glioblastoma) cells (Figure S1). No toxicity was observed in these experiments either. However, the peptides seemed to affect the metabolism of bEnd.3 cells, where a higher proliferation rate was observed (Figure S1B).

Superoxide Anion Scavenging Assay

The superoxide anion scavenging assay was used as an estimation criterion for the antioxidative activity of the designed peptide.

penetration of larger molecules, restricting intracellular delivery of potential therapeutics. Cell-penetrating peptides (CPPs) have the potential to overcome this limitation and are a promising tool to transport molecules across cellular membranes.[21] The ultimate goal is to specifically target organelles to selectively deliver the cargo molecule to the site of action in the cells, either by covalent attachment of the cargo to the CPP or by formation of stable complexes via electrostatic or hydrophobic interactions.[22] Frankel and Pabo[23] and Green and Loewenstein[24] were the first to discover the ability of peptides to penetrate cell membranes in experiments with the HIV-1 trans-activator protein (Tat). Since then, thousands of CPPs have been discovered and studied. Generally, CPPs are composed of 4–30 amino acid residues either net positively charged or with alternating cationic and hydrophobic regions. The main accepted mechanism of CPP uptake is via endocytosis;[25] however, other uptake mechanisms have also been suggested.[26] The mechanism of action has shown strong dependence on the type of CPP, the peptide concentrations, the cargo molecule, and the charge or molar ratio used.

Previously, we have designed a mitochondrial targeting CPP (mtCPP1) composed of D-arginine, 2,6-dimethyl-L-tyrosine, L-ornithine, and L-phenylalanine, described in the N-to-C direction (Figure 1A). The inspiration came from the SS31 peptide, which is a tetrapeptide with alternating aromatic residues and basic amino acids, and we could demonstrate a 2-fold better superoxide anion scavenging ability for mtCPP1 compared with SS31.[27] We have also designed the GSH analog peptide 25 (UPF25) by adding the non-coded amino acid O-methyl-L-tyrosine (Tyr(Me)) to the N terminus, changing the γ-glutamate to α-glutamate, and amidation of the C terminus to GSH (Figure 1B). We have shown that UPF25 has a much higher hydroxyl radical scavenging ability compared with GSH, with a half maximal effective concentration (EC$_{50}$), respectively, of 0.032 ± 0.006 μM and 1231.0 ± 311.8 μM.[28]

Table 1. Library of Synthesized CPPs Used in This Study

Name	Sequence	MW
mtgCPP	D-Arg-Dmt-Orn-Phe-Tyr(Me)-Glu-Cys-Gly-NH$_2$	1091.2
mtCPP1	D-Arg-Dmt-Orn-Phe-NH$_2$	625.4
UPF25	Tyr(Me)-Glu-Cys-Gly-NH$_2$	484.5
FAM-mtgCPP	FAM-D-Arg-Dmt-Orn-Phe-Tyr(Me)-Glu-Cys-Gly-NH$_2$	1449.5
FAM-mtCPP1	FAM-D-Arg-Dmt-Orn-Phe-NH$_2$	983.01
FAM-UPF25	FAM-Tyr(Me)-Glu-Cys-Gly-NH$_2$	842.5

MW, molecular weight; Dmt, 2,6-dimethyl-L-tyrosine; (Me), O-methoxy group; D-, D-form amino acid; Arg, Tyr, Glu, Cys, Gly, Phe, three letter codes for standard L- form amino acids; Orn, L-ornithine.

Figure 2. Effect of Treatment with Peptides at Different Concentrations on HeLa 705 Viability

HeLa 705 cells were treated with mtCPP1, UPF25, and mtgCPP for 24 hr. H$_2$O$_2$ (200 μM and 400 μM) were chosen as positive controls as well as DMSO (20%). Treatment with mtgCPP showed no toxicity. p values obtained from one-way ANOVA multiple comparisons showed no significant difference between each group and untreated cells (complete medium only). Data represent the mean of a minimum of three individual experiments; SD for each data point is shown. Cell viability was quantified by conventional WST-1 assay.

Mitochondrial superoxide was generated as a byproduct of oxidative phosphorylation and detected with a fluorescence method using the MitoSOX Red mitochondrial superoxide indicator as a probe. Analysis of the scavenging ability of peptides showed that the fusion peptide had a remarkably stronger superoxide anion scavenger ability than mtCPP1 and UPF25 alone (Figure 3). The dual antioxidant peptide mtgCPP had an improved superoxide anion scavenging abilities by 2- and 3-fold compared with mtCPP1 and UPF25, respectively. Antimycin A (AMA) was used as positive control because of the ability of the chemical compound to induce an oxidative state in cells. Surprisingly, the covalent conjugation of the mitochondrial peptide to the GSH analog resulted in a more efficient antioxidant CPP, suggesting that both the OH and SH groups are involved in radical depletion reactions. This has been previously investigated by Ehrlich et al.,[29] where the Cys residue in the sequence was replaced with a Ser residue in the UPF26 sequence, and reduction of the hydroxyl radical scavenging ability was not observed. These analogs showed EC$_{50}$ values of the scavenging reaction in the submicromolar range (the EC$_{50}$ for UPF25 was approximately 30 nM).[30]

Mitochondrial Membrane Potential and ATP Production

The chemiosmotic hypothesis postulated by Mitchell[32] describes the process of ATP formation, where the respiratory chain converts redox energy into an electrochemical gradient of protons called proton-motive force (Δp).[31] The two parameters of Δp are the membrane potential (Δψ) and the transmembrane proton gradient (ΔpH), which are thermodynamically equivalent:

$$\Delta p = \Delta \Psi + 2.3 RT / F \Delta pH,$$

where R is the gas constant, T is absolute temperature, and F is Faraday's constant.

The contribution of either parameter to the proton-motive force varies widely in different organisms. In mitochondria, the Δψ component significantly exceeds the ΔpH component and is therefore regarded as the main driving force for ATP production.[33–35]

With the aim of assessing how these antioxidant peptides influence mitochondrial energy provision, Δψ$_m$, and ATP production were studied. Spectrofluorometry analysis using tetramethylrhodamine methyl ester (TMRE) as a fluorescent probe showed that UPF25 influenced the Δψ$_m$. Treatment with UPF25 decreased the Δψ$_m$ in HeLa 705 cells either with or without H$_2$O$_2$ addition. The GSH analog was able to partially rescue the Δψ$_m$ when the cells were under oxidative stress; however, not to the same extent as mtCPP1 and mtgCPP, where results close to the healthy situation were shown. No significant difference was observed between mtCPP1 and mtgCPP, whereas there were significant differences when comparing any of the peptides with untreated cells with addition of H$_2$O$_2$ (Figure 4). ATP production was measured using the firefly luciferin-luciferase assay. The luminescence intensity (L.I.) from HeLa 705 cells after lysis was normalized based on the L.I. of untreated cells. A series of positive and negative controls were used as well. Carbonyl cyanide 4-(trifluoromethoxy)phenylhydrazone (FCCP), a potent mitochondrial oxidative phosphorylation uncoupler able to depolarized Δψ$_m$, was used as a negative control for the Δψ$_m$ measurements. AMA is a chemical compound produced by *Streptomyces* sp., able to bind to mitochondrial complex III blocking mitochondrial electron transfer. This inhibition causes a collapse of the proton gradient across the mitochondrial inner membrane, leading to loss of the Δψ$_m$ and a reduction in the levels of ATP.[36–38] AMA was used as a negative control for the measurement of ATP levels. One-way ANOVA multiple comparisons showed that ATP levels after treatment with mtgCPP and mtCPP1 were similar to the ATP levels of untreated cells (Figure 5).
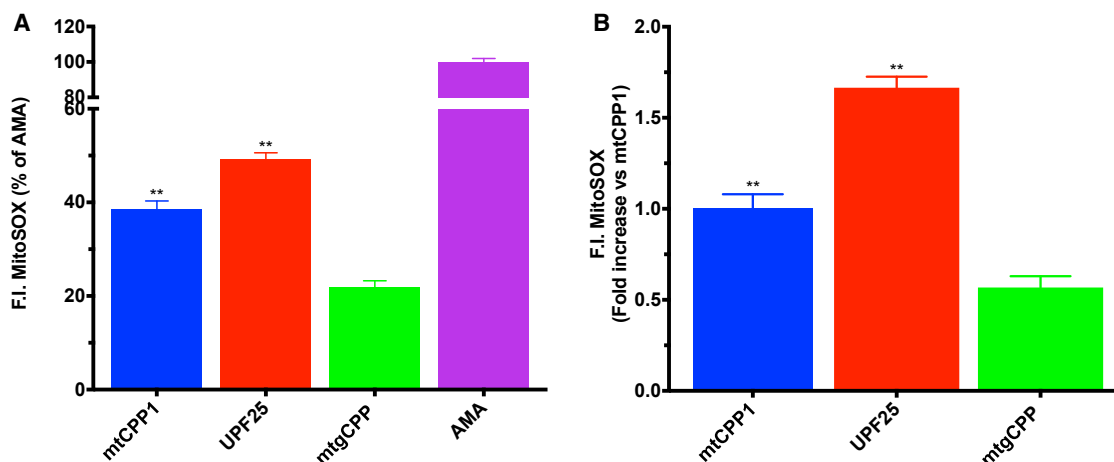
Figure 3. The Superoxide Anion Scavenging Ability of Peptides

(A and B) Superoxide anion levels decreased after treatment with any of the peptides in HeLa 705 cells. Shown are spectrofluorometry data expressing the fluorescence intensity (F.I.) of MitoSOX after 24 hr treatment with peptides at 5 μM concentrations and normalized versus cells treated with AMA as a positive control (A) or versus mtCPP1 superoxide anion scavenging ability (B). Data represent the mean of three individual experiments ± SD. **$p < 0.005$ versus mtCPP1. Superoxide anion levels were measured using the MitoSOX Red mitochondrial superoxide indicator.

The same analysis showed that ATP levels after 24-hr treatment with UPF25 were significantly decreased.

Mechanism of Action of mtgCPP

We proposed a mechanism of superoxide anion scavenging activity (Figure 6) and for the reduction of H_2O_2 (Figure 7) of mtgCPP based on GSH. According to Winterbourn[39] free radical sink, GSH works together with superoxide dismutase to prevent oxidative damage:

$$2O_2^{\leftarrow} + 2H^+ \xrightarrow{\text{Superoxide dismutase}} H_2O_2 + O_2$$

$$R^\bullet + GSH \rightarrow RH + GS^\bullet$$

$$GS^\bullet + GS^- \rightarrow GSSG^{\bullet-}$$

$$GSSG^{\bullet-} + O_2 \rightarrow GSSG + O_2^{\bullet-}.$$
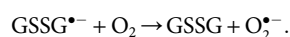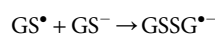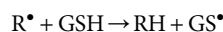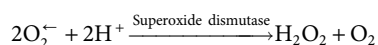
In the same manner, mtgCPP would have a role in protecting cells by catching and neutralizing potentially harmful molecules (Figure 6).

GSH is also used as a substrate for glutathione peroxidase (GSHPx) for the reduction of H_2O_2:

$$H_2O_2 + 2GSH \xrightarrow{\text{Glutathione peroxide}} H_2O + GSSG.$$
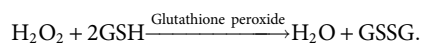
GSH disulfide (GSSG) is reduced to GSH by nicotinamide adenine dinucleotide phosphate (NADPH) through the GSH reductase reaction:

$$GSSG + NADPH + H^+ \xrightarrow{\text{Glutathione reductase}} NADP^+ + 2GSH.$$
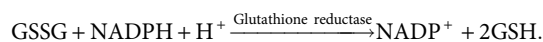
This exchange reaction provides an important mechanism for the action of GSH. Based on these data, we hypothesized and proposed an interconversion mechanism for mtgCPP in its reduced and oxidized form by the action of GSH oxidase, GSH reductase, and GSH peroxidase enzymes (Figure 7).

GSH and molecular oxygen are used as substrates by GSH oxidase in the following reaction:

$$2GSH + O_2 \xrightarrow{\text{Glutathione oxidase}} GSSG + H_2O_2.$$
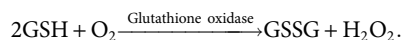
We hypothesized that mtgCPP is capable of preventing damage to cellular compartments caused by ROS acting as GSH in the GSH metabolism.[40]

Microscopic and Spectrofluorometric Analysis of mtgCPP

We have previously shown that mtCPP1 is internalized into cells and is targeting mitochondria. It has also been reported that treatment with GSH or UPFs as well as other GSH analogs does not increase serum GSH levels, mainly because of its rapid degradation and the difficulties with direct uptake into different cell types. It has been shown that the uptake of GSH in cells after 1-hr treatment with 1 mM of GSH was in the low micromolar range (≈ 1.5 μM).[41] To investigate whether mtgCPP follows similar localization as mtCPP1 or whether we could increase the cellular uptake, we attempted to trace the subcellular localization of the internalized peptide by epifluorescence microscopy using organelle-specific fluorescent staining reagents. As shown in Figure 8, mtgCPP as well as mtCPP1 (stained with carboxyfluorescein, green pseudocolor) were found inside cells but not in the nuclei (stained with a Hoechst dye, blue pseudocolor). The mitochondria were stained with a TMRE dye (red pseudocolor), and the orange/yellow pseudocolor resulting from the merged pictures indicated that the peptide partially targets the mitochondria.
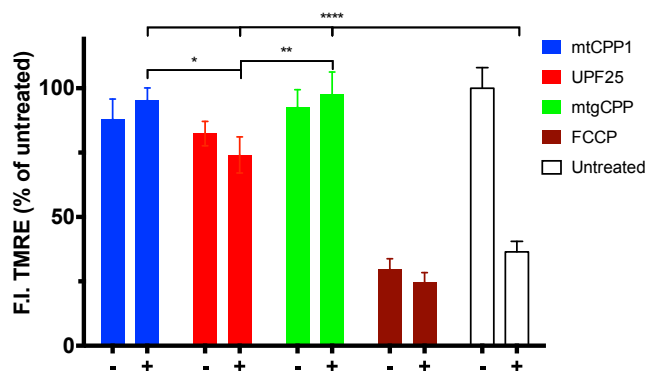
Figure 4. Mitochondrial Membrane Potential

HeLa 705 cells with (+) and without (−) addition of H_2O_2 at 200-μM concentration for 2 hr were treated for 24 hr with peptides at 5 μM concentrations. TMRE fluorescence intensity was measured, and data were recorded from three individual experiments. p values obtained from two-way ANOVA multiple comparisons showed significant differences between mtCPP1 and UPF25 and mtgCPP and UPF25. All peptides were significantly different compared with stressed untreated cells. Data represent the mean ± SD (n = 3). *$p < 0.05$, **$p < 0.005$, ****$p < 0.0005$.

These results, as confirmed during spectrofluorometric analysis, showed that FAM-UPF25 was not internalized. Instead, the fusion peptide was shown to be a CPP entering the cell and accumulating in mitochondria. Similar results were observed when bEnd.3 cells were treated with the peptides at the same concentrations (Figure S2). Spectrofluorometry was used to measure and quantify the subcellular uptake of the fluorescently labeled peptides. Using the procedure to isolate the mitochondria according to the manufacturer's protocol, three different subcellular fractions were obtained: membranes (plasma membrane and nuclear membrane), cytosol, and mitochondria. We determined the carboxyfluorescein fluorescence intensities in the three fractions after treatment with peptides for 24 hr in HeLa 705 cells. FAM-mtgCPP was presented in the membranes to the same extent as FAM-mtCPP1, whereas FAM-UPF25 was registered to accumulate in the membranes four times higher than the other two peptides (Figure 9A). Interestingly, the fluorescence signal from FAM-mtgCPP was found to be 8- and 19-fold higher than that of FAM-mtCPP1 and FAM-UPF25, respectively, in the cytosol fraction (Figure 9B). Only a 2-fold increase was observed between FAM-UPF25 and FAM-mtCPP1. Moreover, the data showed that FAM-mtgCPP is mainly accumulated in the mitochondria. The uptake of FAM-mtgCPP was 10- and 33-fold higher than that of FAM-mtCPP1 and FAM-UPF25, respectively (Figure 9C).

Peptide Characterization

Sizes and zeta potentials of mtgCPP were determined using a Zetasizer machine. The peptide exhibited a size of 150 and 400 nm in diameter when dissolved in MilliQ H_2O or in cell culture media at 5 μM final concentration, respectively (Table S1). This means that the peptide is forming aggregates because an eight amino acid-long peptide would not have a similar size. The zeta potentials of mtgCPP were mainly electropositive at all of the different tested concentra-
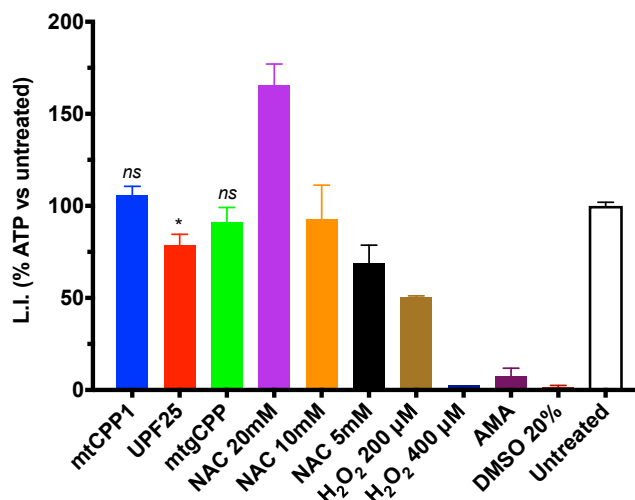
Figure 5. ATP Levels after Treatment with Peptides

ATP levels in HeLa 705 were measured 24 hr after treatment with peptides and controls. The luminescence intensity (L.I.) was normalized to the untreated cells level in each individual well. mtgCPP did not show a difference in ATP production compared with untreated cells. Data represent the mean of three experiments ± SD for each data point. p values were obtained from ordinary one-way ANOVA multiple comparisons (*$p < 0.0001$). ATP levels were measured by firefly luciferin-luciferase luminescence assay.

tions, as expected from the nature of a peptide consisting of an excess of positively charged amino acids (Table S1).

Here we present a novel antioxidant cell-penetrating peptide. We studied the toxicity of the designed peptide and found that mtgCPP did not affect the viability of several different cell lines even at 100 μM concentration. The non-toxic influence of the peptide was also confirmed by studying the functionality of the mitochondria after treatment. We investigated the $\Delta\psi_m$ and ATP production. A depolarization of the $\Delta\psi_m$ was recorded after treatment with H_2O_2 at 200 μM concentration to induce the oxidative stress. Treatment with mtgCPP was able to rescue the $\Delta\psi_m$ at the same level as the untreated cells without addition of H_2O_2. Measurements of ATP production showed that the ATP levels of cells treated with any of the peptides were similar to the ATP levels of untreated cells. We have shown that the fused peptide, mtgCPP, prevented ROS formation with lower mitochondrial superoxide levels in cells compared with treatment with one of the peptides alone. A significant 2- and 3-fold decrease of ROS levels were recorded for mtgCPP compared to mtCPP1 and UPF25, respectively. The microscopy studies showed the internalization of mtgCPP into HeLa 705 and bEnd.3 cells. These data suggest that part of the synergistic antioxidative activity might be a result of the ability of mtCPP1 fragments to carry into cells UPF25 fragments at a higher concentration. The spectrofluorometric analysis of different cellular compartments using fluorescein-conjugated peptides gave unexpected results. We did not expect to find a better targeting ability of the new CPP compared with the parent mitochondrial peptide because a mitochondrial targeting ability of the GSH
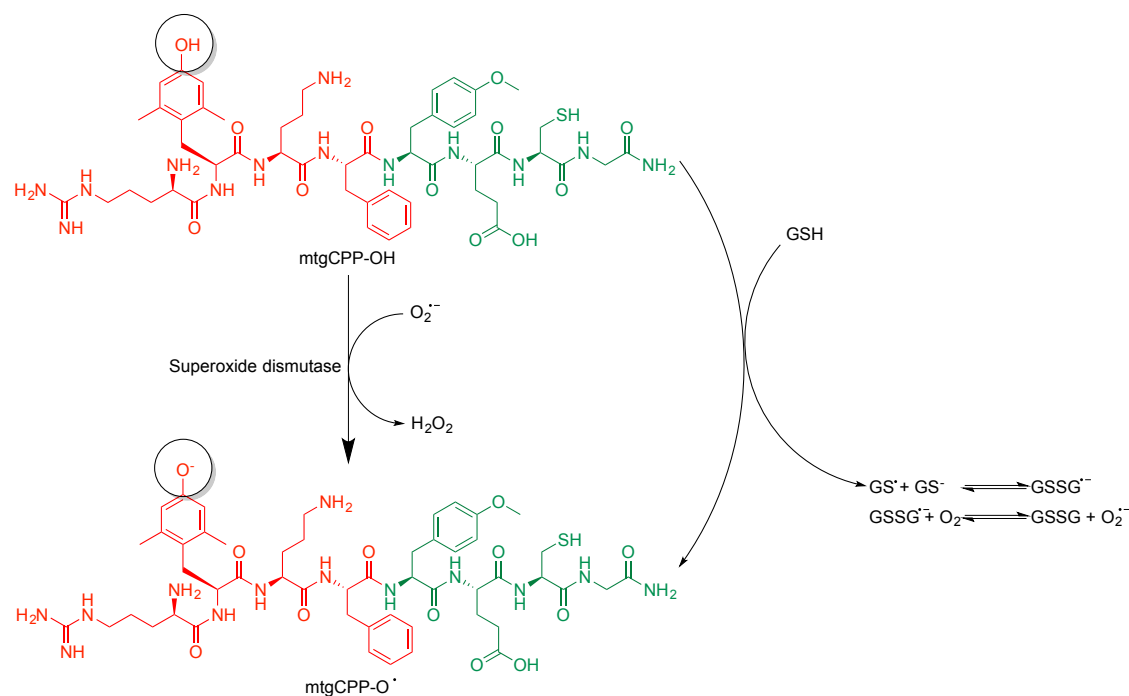
Figure 6. Proposed Mechanism of Superoxide Anion Scavenging Activity of mtgCPP

analog peptide has not been shown. There were 10- and 33-fold increases in FAM-mtgCPP uptake in the mitochondria and 8- and 19-fold increases in uptake in the cytosol compared with FAM-mtCPP1 and FAM-UPF25, respectively. Even though mtgCPP accumulated to such a higher extent compared with the other peptides, antioxidant activity was only improved by 2- to 3-fold. In conclusion, our data suggest an additive synergistic effect of mtgCPP on scavenging of free radicals in live cells.

The compounds discussed in this study may also act by regulating other pathways along with antioxidative mechanisms, which may result in synergistic antioxidative effects. In addition, combinatorial therapy with antioxidants should be considered, where they are combined with existing drugs. This might be a way to enhance the efficacy of standard therapy in the treatment of different diseases, like cardiovascular and neurodegenerative diseases. To achieve this result, a complete understanding of the molecular mechanisms of the ROS specificities in each disease and in each state of the disease as well as animal studies and clinical trials are needed to confirm these antioxidative beneficial effects.

MATERIALS AND METHODS
Design, Synthesis, Purification, and Analysis of Peptides
All peptides were designed based on our previously published peptides, mtCPP1 and UPF25.[27,28] Peptides were synthesized in stepwise manner in a 0.1 mmol scale on a Biotage Alstra Plus peptide synthesizer (Biotage) using a fluorenylmethyloxycarbonyl (fmoc) solid-phase peptide synthesis (SPPS) strategy with ChemMatrix

Rink Amide resin (0.45 mmol/g) as a solid support to obtain C-terminally amidated peptides.[30] The resin was swollen in N,N-dimethylformamide (DMF) for 20 min at 70°C with an oscillating mixer. At each coupling step, fmoc-protected D- or L-amino acids were used and dissolved in DMF, and ethyl 2-cyano-2-(hydroxyimino)acetate (OxymaPure) and carbodiimide (DIC) were used as coupling reagents for 5 min at 75°C (Table S1). The fmoc group was removed by treatment with piperidine (20% v/v) in DMF (first reaction at 45°C for 2 min and the second reaction at room temperature for 12 min). The final cleavage was performed using a standard protocol (95% trifluoroacetic acid [TFA], 2.5% triisopropylsilane [TIS], and 2.5% H$_2$O) for 4 hr at room temperature. Peptides were precipitated in cold diethyl ether and purified by reverse-phase high-performance liquid chromatography (RP-HPLC) using a BioBasic C-8 column (Thermo Scientific) and a 20%–80% acetonitrile (in water with addition of 0.1% TFA to both solvents) gradient. The purified peptides were lyophilized, and the molecular masses of the peptides were analyzed by ultra-performance liquid chromatography-mass spectrometer (UHPLC-MS; Agilent 1260 Infinity, Agilent Technologies).

Cell Culture
HeLa 705 cells (a human cervical carcinoma cell line) were grown in DMEM with Glutamax supplemented with 0.1 mM non-essential amino acid solution, 100 U/mL penicillin, 100 μg/mL streptomycin, and 10% fetal bovine serum (FBS). bEnd.3 cells (a mouse brain endothelial cell line) and CHO cells were grown in DMEM with Glutamax supplemented with 3 mM L-glutamine, 100 U/mL penicillin,
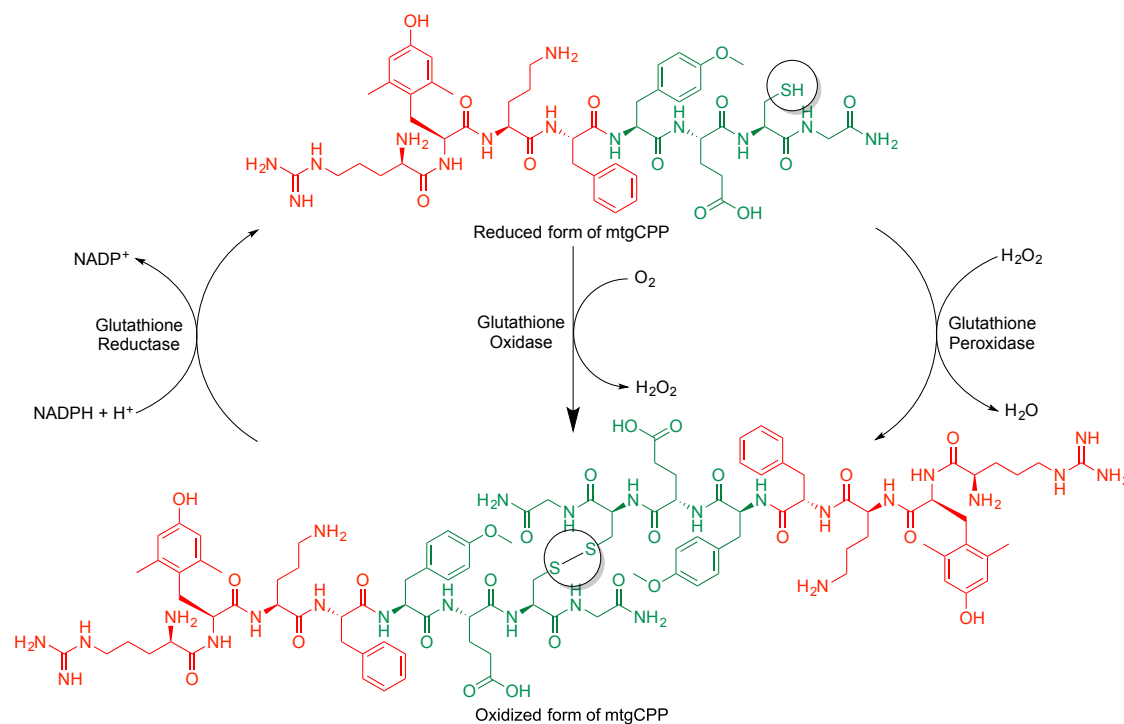
Figure 7. Proposed Interconversion of mtgCPP in Its Reduced Form and Oxidized Form by the Action of Glutathione Oxidase, Glutathione Reductase, and Glutathione Peroxidase Enzymes

100 μg/mL streptomycin, and 10% FBS. U87 cells (a human primary glioblastoma cell line) were grown in DMEM with Glutamax supplemented with 100 U/mL penicillin, 100 μg/mL streptomycin, and 10% FBS. Cells were cultured at 37°C in a 5% CO_2 atmosphere. All media and chemicals were purchased from Invitrogen.

Cell Proliferation Assay

Cell proliferation was determined by using the WST-1 cell proliferation assay (Roche Diagnostics) according to the manufacturer's instructions. Briefly, HeLa 705, bEnd.3, U87, and CHO cells were seeded at 7×10^3 cells/well into 96-well plates 24 hr prior to experiments. The cells were treated with peptides at different concentrations and incubated for 24 hr in complete growth medium according to the cell line. WST-1 cell proliferation reagent was added after 20 hr of peptide treatment to each well at a final dilution of 1:10. After 4 hr incubation, the plate was placed on a Sunrise microplate absorbance reader (Tecan) and shaken for 1 min before the reading, and absorbance of the formazan product was then measured at 450 nm. The reference wavelength used was 650 nm. Cells incubated for 24 hr with 20% DMSO in complete media (v/v) were used as positive control as well as cells treated with H_2O_2 200 μM and 400 μM concentration.

Δψm Assay

$\Delta\psi_m$ was evaluated using the fluorescent probe TMRE (mitochondrial potential membrane assay kit, Abcam). The positively charged cell-permeant dye TMRE readily accumulates in active mitochondria because of their relative negative charge. The dye fails to be sequestered into depolarized and/or non-functional mitochondria because of a decrease in $\Delta\psi_m$. Briefly, HeLa 705 cells were seeded into 96-well plates 24 hr before the treatments. Cells were treated with peptides for 24 hr at different concentrations as previously described. H_2O_2 (200 μM) was used as a positive control. TMRE (400 nM) was added to the complete medium, and cells were incubated for 30 min at 37°C, 5% CO_2 and protected from light. The medium was removed, and cells were washed once with PBS to remove background fluorescence from the cell culture medium. 100 μL/well of 0.2% BSA in PBS was added. The plate was read on a fluorescence reader (peak excitation = 549 nm, peak emission = 575 nm). The same assay was performed to evaluate the ability of peptides to restore a physiological $\Delta\psi_m$ after insult with H_2O_2. Briefly, cells were plated and treated with peptides at different concentrations as previously described. After 2 hr of exposure to 200 μM H_2O_2, cells were incubated for 24 hr at 37°C and 5% CO_2. Medium containing TMRE was prepared and added to each well at 400 nM final concentration. Cell medium was removed after 30 min, and cells were washed once with PBS and replaced with 100 μL/well of 0.2% BSA in PBS. The $\Delta\psi_m$ was measured by spectrofluorescence reader (Flex Station II, Molecular Devices; peak excitation = 549 nm, peak emission = 575 nm). The $\Delta\psi_m$ of treated cells was expressed as the percentage of $\Delta\psi_m$ of untreated cells or of untreated cells with addiction of H_2O_2 at 200 μM concentration.
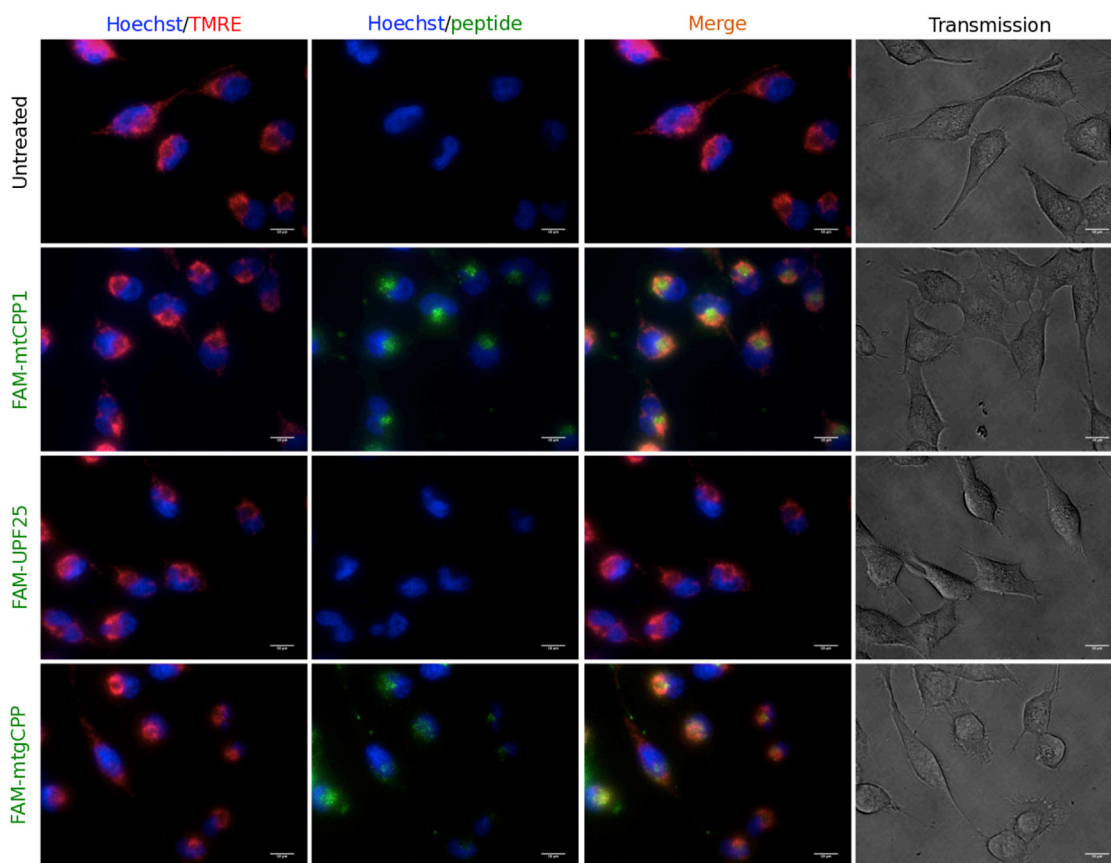
Figure 8. Cellular Uptake and Localization of FAM-mtCPP1, FAM-UPF25, and FAM-mtgCPP in HeLa 705 Cells

Cells were incubated with peptides at 5 μM concentration for 4 hr before imaging. 200 nM TMRE was added 30 min before images were acquired. Hoechst 33342 was added at 1 μg/mL for 10 min before images were acquired. Untreated cells were kept under the same condition as treated cells without any peptide treatment. Fresh complete growth medium was added when the peptides were added to the other samples. Green pseudocolor corresponds to carboxyfluorescein-conjugated peptides. Red pseudocolor corresponds to TMRE, a mitochondrial dye. Blue pseudocolor corresponds to Hoechst 33342, a nuclear dye. Merged images show the extent of mitochondrial localization for the peptides. Scale bars, 10 μm.

Superoxide Anion Scavenging Assay

ROS production was determined by using the fluorescent probe MitoSOX Red mitochondrial superoxide indicator (Invitrogen Detection Technologies). MitoSOX Red reagent is rapidly and selectively targeted to mitochondria. When in mitochondria, MitoSOX Red reagent is oxidized by superoxide and exhibits red fluorescence (Life Technologies, Molecular Probes). According to the manufacturer's protocol, a vial of MitoSOX reagent was dissolved in 13 μL of DMSO to make a 5 mM MitoSOX reagent stock solution. The 5 mM stock solution was diluted in Hank's balanced salt solution (HBSS)/Ca/Mg to obtain a 5 μM MitoSOX reagent working solution. Briefly, HeLa 705 and bEnd.3 cells were seeded in 96-well plates at a concentration of 7×10^3 cells/well containing 100 μL of complete medium and allowed to recover for 24 hr. Cells were treated with peptides at 5 μM concentration for 24 hr. MitoSOX reagent 5 μM was added to the cells, and they were incubated for 10 min at 37°C and 5% CO_2, protected from light. After staining with MitoSOX, the medium was aspirated, and the cells were washed once with 0.2% BSA in

PBS to remove background fluorescence, and finally 100 μL/well of 0.2% BSA in PBS was added. The plate was read with a fluorescence reader (Flex Station II, Molecular Devices) with settings suitable for MitoSOX (peak excitation = 510 nm, peak emission = 580 nm).

Isolation of Mitochondria

The compartmentalization of the peptides inside the cells was determined using the Thermo Scientific mitochondrial isolation kit for cultured cells. The kit enables the isolation of intact mitochondria from cultured mammalian cells. The protocol relies on a reagent-based method and differential centrifugation to separate the mitochondrial and cytosolic fractions. Briefly, HeLa 705 cells were grown in 225 cm² flasks and allowed to recover for 24 hr. Cells were treated with fluorescein-conjugated peptides at 5-μM concentration for 24 hr. Cells reached 90% confluence with an average cell yield of 2.25×10^7 and were harvested using a cell scraper (Sarstedt). The flask was washed with 10 mL fresh complete medium, transferred to a 15-mL Falcon tube, and centrifuged at ~850 × g for 2 min.
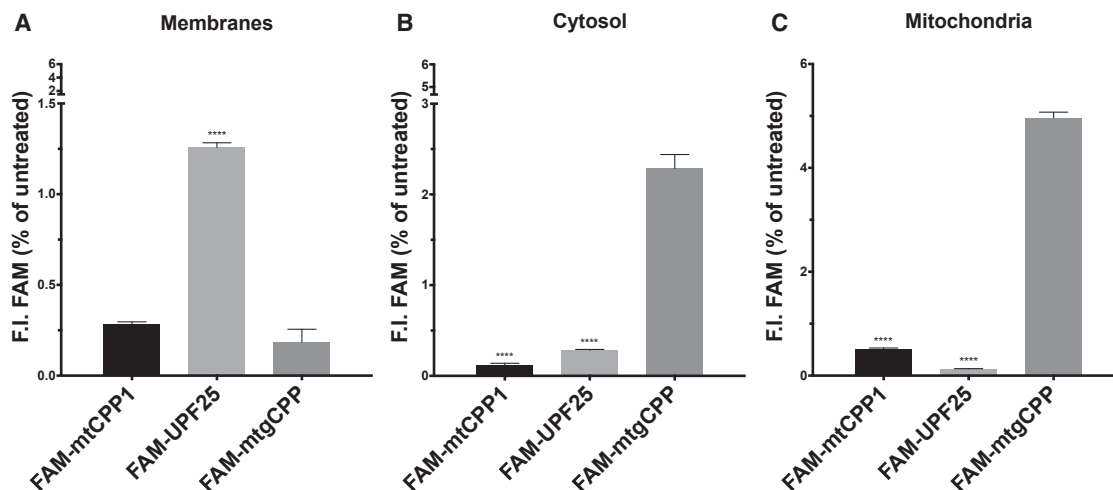
Figure 9. Uptake of Fluorescein-Conjugated Peptides in Different Cellular Compartments

(A–C) Uptake of FAM-mtCPP1, FAM-UPF25, and FAM-mtgCPP after 24 hr treatment with peptides at 5 μM concentration in (A) membranes, (B) cytosol, and (C) isolated mitochondria fractions from HeLa 705 cells. FAM-UPF25 mainly accumulates in membranes with a fluorescence intensity (F.I.) 4-fold higher than the F.I. of FAM-mtCPP1 and FAM-mtgCPP. In the cytosol and in mitochondria, FAM-mtgCPP accumulates to a higher extent than FAM-mtCPP1 and FAM-UPF25; 8- and 19-fold and 10- and 33-fold, respectively. The F.I. was normalized to the untreated cells level. Data represent the mean of three individual experiments ± SD for each data point. p values were obtained from ordinary one-way ANOVA multiple comparisons. ****$p < 0.0001$.

The supernatant was removed and discarded. The pellet was suspended in 1.5 mL medium and centrifuged at ~850 × g for 2 min. The supernatant was removed and discarded. 800 μL of mitochondrion isolation reagent A was added and vortexed at medium speed for 5 s, and the tube was incubated on ice for exactly 2 min. 10 μL of mitochondrion isolation reagent B was added and vortexed at maximum speed for 5 s. The tube was incubated on ice for 5 min, vortexing at maximum speed every minute. 800 μL of mitochondrion isolation reagent C was added, and the tube was inverted several times to mix. The tube was centrifuged at 700 × g for 10 min at 4°C. The supernatant was transferred to a new 2.0-mL tube and centrifuged at 12,000 × g for 15 min at 4°C. The supernatant (cytosol fraction) was transferred to a new tube. The pellet contained the isolated mitochondria. 500 μL of mitochondrion isolation reagent C was added to the pellet and centrifuged at 12,000 × g for 5 min. The supernatant was removed and discarded. After the isolation, the mitochondria were resuspended in complete medium, and 100 μL/well were transferred in a black clear-bottom 96-well plate. The plate was immediately read with a fluorescence reader (Flex Station II, Molecular Devices) with settings suitable for fluorescein (excitation, 510 nm; emission, 580 nm).

Fluorescence Microscopy

The digital images were obtained with an inverted fluorescence microscope LSM Pascal (Zeiss) at 2,048 × 2,048 pixels. Images were taken using 10× and 40× dry objective lenses and a 63× oil immersion objective lens, and the optical section was <1 μm. Fluorescence was excited for Hoechst 33342 and FAM by the 346- and 494-nm line of an argon laser, and emission at 497 and 519 nm was recorded, respectively, for the nuclear and peptide stains. To localize mitochon-

dria, cells were loaded with 200 nM TMRE, which distributes into negatively charged cellular compartments, for 20 min at 37°C. TMRE fluorescence was excited by laser at 535 nm and recorded at 575 nm. A blue pseudocolor was applied to visualize the nuclear stain. Green and red pseudocolors were applied to visualize the localization of peptide into cells and mitochondria. All recordings were performed at controlled temperatures (36°C ± 1°C). Images were analyzed with the software program ImageJ.

ATP Assay

The ATP measurements were performed on HeLa 705 cells. ATP was determined by using an ATP determination assay. The quantitative determination of ATP was assessed using recombinant firefly luciferase and its substrate D-luciferin. The assay was based on luciferase's requirement for ATP in producing light. All other reagents, magnesium sulfate ($MgSO_4$), Tricine, DTT, coenzyme A (CoA), EDTA, sodium azide, and ATP were bought from Sigma-Aldrich. For the luciferase assay, a standard reaction solution was prepared containing distilled water (dH_2O), 20× reaction buffer (500 mM Tricine buffer [pH 7.8], 100 mM $MgSO_4$, 2 mM EDTA, and 2 mM sodium azide), 0.1 M DTT, 10 mM D-luciferin, and firefly luciferase (5 mg/mL) stock solution. ATP was diluted serially in the standard reaction solution, and a standard curve was generated. To assess the intracellular ATP, HeLa 705 cells were seeded 24 hr before treatment with the peptide in white-walled 96-well plates. Cells were treated for 24 hr, and cell medium was removed. Then, 20 μL of cell lysis buffer was added and incubated for 10 min at room temperature. Standard reaction solution was added, and, immediately, light emissions were acquired for approximately 30 s using a GLOMAX 96 microplate luminometer (Promega).

Dynamic Light Scattering

Dynamic light scattering (DLS) was used to determine the hydrodynamic mean diameter and the zeta potential of mtgCPP. The peptide was dissolved in DMEM (Invitrogen) supplemented with 10% FBS or MilliQ water with pH adjusted to 7.4. Measurements were carried out using a Zetasizer Nano ZS apparatus (Malvern Instruments). Samples were assessed in disposable low-volume cuvettes. All data were plotted as size distribution by intensity.

Statistical Analysis

Statistical significance of data was assessed by one-way or two-way ANOVA as appropriate, performed using GraphPad Prism software v. 6.0h (GraphPad). All values are represented as mean ± SD. p values considered significant are indicated in each figure.

SUPPLEMENTAL INFORMATION

Supplemental Information includes two figures and one table and can be found with this article online at http://dx.doi.org/10.1016/j.omtm.2017.04.010.

AUTHOR CONTRIBUTIONS

Conceptualization, C.P.C. and Ü.L.; Methodology, C.P.C.; Investigation, C.P.C.; Writing, C.P.C.; Funding Acquisition, Ü.L.; Supervision, Ü.L.

CONFLICTS OF INTEREST

The authors declare no conflict of interest.

ACKNOWLEDGMENTS

REFERENCES

1. Flannagan, R.S., Cosío, G., and Grinstein, S. (2009). Antimicrobial mechanisms of phagocytes and bacterial evasion strategies. Nat. Rev. Microbiol. 7, 355–366.

2. Nakabeppu, Y., Tsuchimoto, D., Ichinoe, A., Ohno, M., Ide, Y., Hirano, S., Yoshimura, D., Tominaga, Y., Furuichi, M., and Sakumi, K. (2004). Biological significance of the defense mechanisms against oxidative damage in nucleic acids caused by reactive oxygen species: from mitochondria to nuclei. Ann. N Y Acad. Sci. 1011, 101–111.

3. Reddy, V.P., Beyaz, A., Perry, G., Cooke, M.S., Sayre, L.M., and Smith, M.A. (2007). The Role of Oxidative Damage to Nucleic Acids in the Pathogenesis of Neurological Disease. Oxidative Damage to Nucleic Acids (Springer New York), pp. 123–140.

4. Imlay, J.A. (2013). The molecular mechanisms and physiological consequences of oxidative stress: lessons from a model bacterium. Nat. Rev. Microbiol. 11, 443–454.

5. Ayala, A., Muñoz, M.F., and Argüelles, S. (2014). Lipid peroxidation: production, metabolism, and signaling mechanisms of malondialdehyde and 4-hydroxy-2-nonenal. Oxid. Med. Cell. Longev. 2014, 360438.

6. Costantini, P., Jacotot, E., Decaudin, D., and Kroemer, G. (2000). Mitochondrion as a novel target of anticancer chemotherapy. J. Natl. Cancer Inst. 92, 1042–1053.

7. Wu, G., Fang, Y.Z., Yang, S., Lupton, J.R., and Turner, N.D. (2004). Glutathione metabolism and its implications for health. J. Nutr. 134, 489–492.

8. Forman, H.J. (2016). Glutathione - From antioxidant to post-translational modifier. Arch. Biochem. Biophys. 595, 64–67.

9. Brewer, M.S. (2011). Natural Antioxidants: Sources, Compounds, Mechanisms of Action, and Potential Applications. Compr. Rev. Food Sci. Food Saf. 10, 221–247.

10. Lushchak, V.I. (2011). Adaptive response to oxidative stress: Bacteria, fungi, plants and animals. Comp. Biochem. Physiol. Part C Toxicol. Pharmacol. 153, 175–190.

11. Arlt, S., Müller-Thomsen, T., and Beisiegel, U. (2002). Use of Vitamin C and E in the Treatment of Alzheimer's Disease. Drug Dev. Res. 56, 452–457.

12. Allen, J., and Bradley, R.D. (2011). Effects of oral glutathione supplementation on systemic oxidative stress biomarkers in human volunteers. J. Altern. Complement. Med. 17, 827–833.

13. Schmitt, B., Vicenzi, M., Garrel, C., and Denis, F.M. (2015). Effects of N-acetylcysteine, oral glutathione (GSH) and a novel sublingual form of GSH on oxidative stress markers: A comparative crossover study. Redox Biol. 6, 198–205.

14. Ribas, G.S., Vargas, C.R., and Wajner, M. (2014). L-carnitine supplementation as a potential antioxidant therapy for inherited neurometabolic disorders. Gene 533, 469–476.

15. Mathew, M.C., Ervin, A.-M., Tao, J., and Davis, R.M. (2012). Antioxidant vitamin supplementation for preventing and slowing the progression of age-related cataract. Cochrane Database Syst. Rev. 6, CD004567.

16. Steinhubl, S.R. (2008). Why have antioxidants failed in clinical trials? Am. J. Cardiol. 101 (10A), 14D–19D.

17. Goodman, M., Bostick, R.M., Kucuk, O., and Jones, D.P. (2011). Clinical trials of antioxidants as cancer prevention agents: past, present, and future. Free Radic. Biol. Med. 51, 1068–1084.

18. Mecocci, P., and Polidori, M.C. (2012). Antioxidant clinical trials in mild cognitive impairment and Alzheimer's disease. Biochim. Biophys. Acta. 1822, 631–638.

19. Poljsak, B., Šuput, D., and Milisav, I. (2013). Achieving the balance between ROS and antioxidants: when to use the synthetic antioxidants. Oxid. Med. Cell. Longev. 2013, 956792.

20. Poljsak, B. (2011). Strategies for reducing or preventing the generation of oxidative stress. Oxid. Med. Cell. Longev. 2011, 194586.

21. Cerrato, C.P., Künnapuu, K., and Langel, Ü. (2017). Cell-penetrating peptides with intracellular organelle targeting. Expert Opin. Drug Deliv. 14, 245–255.

22. Cerrato, C.P., Lehto, T., and Langel, Ü. (2014). Peptide-based vectors: recent developments. Biomol. Concepts 5, 479–488.

23. Frankel, A.D., and Pabo, C.O. (1988). Cellular uptake of the tat protein from human immunodeficiency virus. Cell 55, 1189–1193.

24. Green, M., and Loewenstein, P.M. (1988). Autonomous functional domains of chemically synthesized human immunodeficiency virus tat trans-activator protein. Cell 55, 1179–1188.

25. Madani, F., Lindberg, S., Langel, U., Futaki, S., and Gräslund, A. (2011). Mechanisms of cellular uptake of cell-penetrating peptides. J. Biophys. 2011, 414729.

26. Räägel, H., Hein, M., Kriiska, A., Säälik, P., Florén, A., Langel, Ü., and Pooga, M. (2013). Cell-penetrating peptide secures an efficient endosomal escape of an intact cargo upon a brief photo-induction. Cell. Mol. Life Sci. 70, 4825–4839.

27. Cerrato, C.P., Pirisinu, M., Vlachos, E.N., and Langel, Ü. (2015). Novel cell-penetrating peptide targeting mitochondria. FASEB J. 29, 4589–4599.

28. Ehrlich, K., Viirlaid, S., Mahlapuu, R., Saar, K., Kullisaar, T., Zilmer, M., Langel, U., and Soomets, U. (2007). Design, synthesis and properties of novel powerful antioxidants, glutathione analogues. Free Radic. Res. 41, 779–787.

29. Ehrlich, K., Ida, K., Mahlapuu, R., Kairane, C., Oit, I., Zilmer, M., and Soomets, U. (2009). Characterization of UPF peptides, members of the glutathione analogues library, on the basis of their effects on oxidative stress-related enzymes. Free Radic. Res. 43, 572–580.

30. Soomets, U., Zilmer, M., and Langel, U. (2005). Manual solid-phase synthesis of glutathione analogs: a laboratory-based short course. Methods Mol. Biol. 298, 241–257.

31. Wallace, D.C. (1999). Mitochondrial diseases in man and mouse. Science 283, 1482–1488.

32. Mitchell, P. (2011). Chemiosmotic coupling in oxidative and photosynthetic phosphorylation. Biochim Biophys Acta. 1807, 1507–1538.

33. Dimroth, P., Kaim, G., and Matthey, U. (2000). Crucial role of the membrane potential for ATP synthesis by F(1)F(o) ATP synthases. J. Exp. Biol. *203*, 51–59.

34. Ramzan, R., Staniek, K., Kadenbach, B., and Vogt, S. (2010). Mitochondrial respiration and membrane potential are regulated by the allosteric ATP-inhibition of cytochrome c oxidase. Biochim Biophys Acta. *1797*, 1672–1680.

35. Vojtísková, A., Jesina, P., Kalous, M., Kaplanová, V., Houstek, J., Tesarová, M., Fornůsková, D., Zeman, J., Dubot, A., and Godinot, C. (2004). Mitochondrial membrane potential and ATP production in primary disorders of ATP synthase. Toxicol. Mech. Methods *14*, 7–11.

36. Alexandre, A., and Lehninger, A.L. (1984). Bypasses of the antimycin A block of mitochondrial electron transport in relation to ubisemiquinone function. Biochem Biophys Acta. *767*, 120–129.

37. Pham, N.A., Robinson, B.H., and Hedley, D.W. (2000). Simultaneous detection of mitochondrial respiratory chain activity and reactive oxygen in digitonin-permeabilized cells using flow cytometry. Cytometry *41*, 245–251.

38. Balaban, R.S., Nemoto, S., and Finkel, T. (2005). Mitochondria, oxidants, and aging. Cell *120*, 483–495.

39. Winterbourn, C.C. (1993). Superoxide as an intracellular radical sink. Free Radic. Biol. Med. *14*, 85–90.

40. Deponte, M. (2013). Glutathione catalysis and the reaction mechanisms of glutathione-dependent enzymes. Biochim. Biophys. Acta *1830*, 3217–3266.

41. Kovacs-Nolan, J., Rupa, P., Matsui, T., Tanaka, M., Konishi, T., Sauchi, Y., Sato, K., Ono, S., and Mine, Y. (2014). In vitro and ex vivo uptake of glutathione (GSH) across the intestinal epithelium and fate of oral GSH after in vivo supplementation. J. Agric. Food Chem. *62*, 9499–9506.